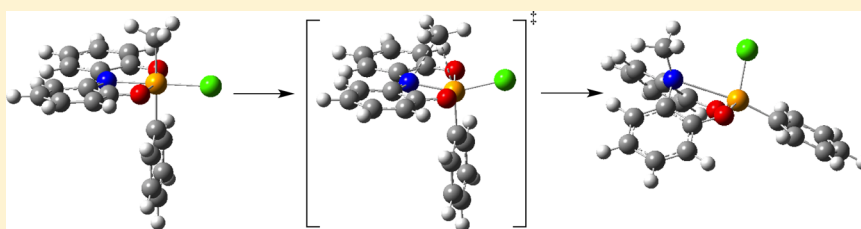


# Mechanism and Selectivity of Methyl and Phenyl Migrations in Hypervalent Silylated Iminoquinones

Sukesh Shekar and Seth N. Brown\*

Department of Chemistry and Biochemistry, University of Notre Dame, 251 Nieuwland Science Hall, Notre Dame, Indiana 46556-5670, United States

## Supporting Information



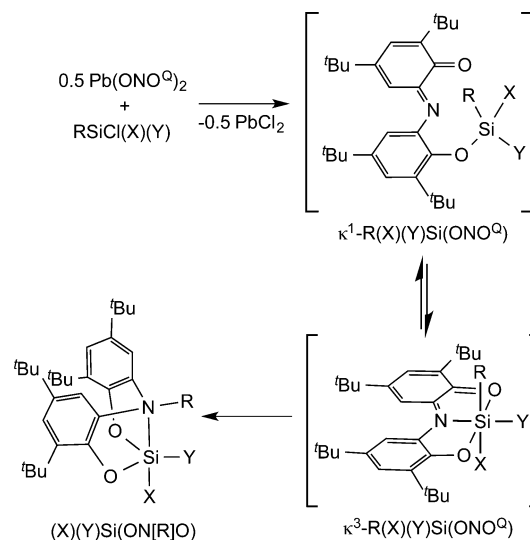
**ABSTRACT:** Chlorosilanes  $R(X)(Y)SiCl$  ( $R = Me, Ph$ ;  $X, Y = Me, Ph, Cl$ ) have been reported to react with  $Pb(ONO^Q)_2$  ( $ONO^Q = 3,5$ -di-*tert*-butyl-1,2-quinone-(3,5-di-*tert*-butyl-2-oxy-1-phenyl)imine) to give five-coordinate  $(X)(Y)Si(ON[R]O)$ , in which the  $R$  group has migrated from silicon to nitrogen. This migration is intramolecular, as confirmed by the lack of crossover between  $(CH_3)_3SiCl$  and  $(CD_3)_3SiCl$  in their reaction with  $Pb(ONO^Q)_2$ . Reaction of  $PhSiMeCl_2$  takes place with high kinetic stereoselectivity to produce isomer  $Ph(Cl)Si(ON[Me]O)$  in which the phenyl is axial in the trigonal bipyramid, which subsequently isomerizes to the thermodynamic isomer with axial chlorine. This indicates that migration takes place preferentially from the stereoisomer of the octahedral intermediate,  $\kappa^3$ - $Ph(CH_3)(Cl)Si(ONO^Q)$ , in which the phenyl and methyl groups are mutually trans, indicating that the observed complete selectivity for methyl over phenyl migration is due to intrinsic differences in migratory aptitude. DFT calculations suggest that migration takes place from this isomer not because it undergoes migration faster than other possible stereoisomers, but because it is formed most rapidly, and migration occurs faster than isomerization.

## INTRODUCTION

The silicon–carbon bond is an important functional group in organic chemistry. Normally, its lack of reactivity is crucial, allowing, for instance, the ubiquitous use of trialkylsilyl groups as protecting groups.<sup>1</sup> However, it is now widely recognized that the formation of hypervalent silicon species, typically by the addition of strong silicophilic Lewis bases such as fluoride, greatly enhances the reactivity of alkyl-, alkenyl-, and arylsilanes.<sup>2</sup> Because organosilanes are inexpensive, nontoxic, and readily handled, this strategy has been broadly used in reactions to form carbon–carbon<sup>3</sup> and carbon–oxygen<sup>4</sup> bonds.

We recently reported that silylation of the oxidized ligand in  $Pb(ONO^Q)_2$  ( $ONO^Q = 3,5$ -di-*tert*-butyl-1,2-quinone-(3,5-di-*tert*-butyl-2-oxy-1-phenyl)imine) with a variety of chlorosilanes  $R(X)(Y)SiCl$  ( $R = Me, Ph$ ;  $X, Y = Me, Ph, Cl$ ) results in tetracyclic, trigonal bipyramidal compounds  $(X)(Y)Si(ON[R]O)$  ( $X = axial, Y = equatorial$ ) with a reduced, dianionic amine-bisphenolate ligand in which the methyl or phenyl group has migrated to nitrogen.<sup>5</sup> The reduced nitrogen donor of the amine-bisphenolate binds to the silicon in the axial position, and a complete preference for migration of the methyl over the phenyl group is observed. A basic outline of this mechanism is given in Scheme 1. Presumably, the reaction is initiated by silylation at the oxygen of  $Pb(ONO^Q)_2$  to produce a siloxyaryliminoquinone,  $\kappa^1$ - $R(X)(Y)Si(ONO^Q)$ , containing four-coordinate silicon. Silicon–carbon bond cleavage in this

## Scheme 1. Proposed Mechanism of Silylation of $Pb(ONO^Q)_2$ To Give Pentacoordinate Products $(X)(Y)Si(ON[R]O)$

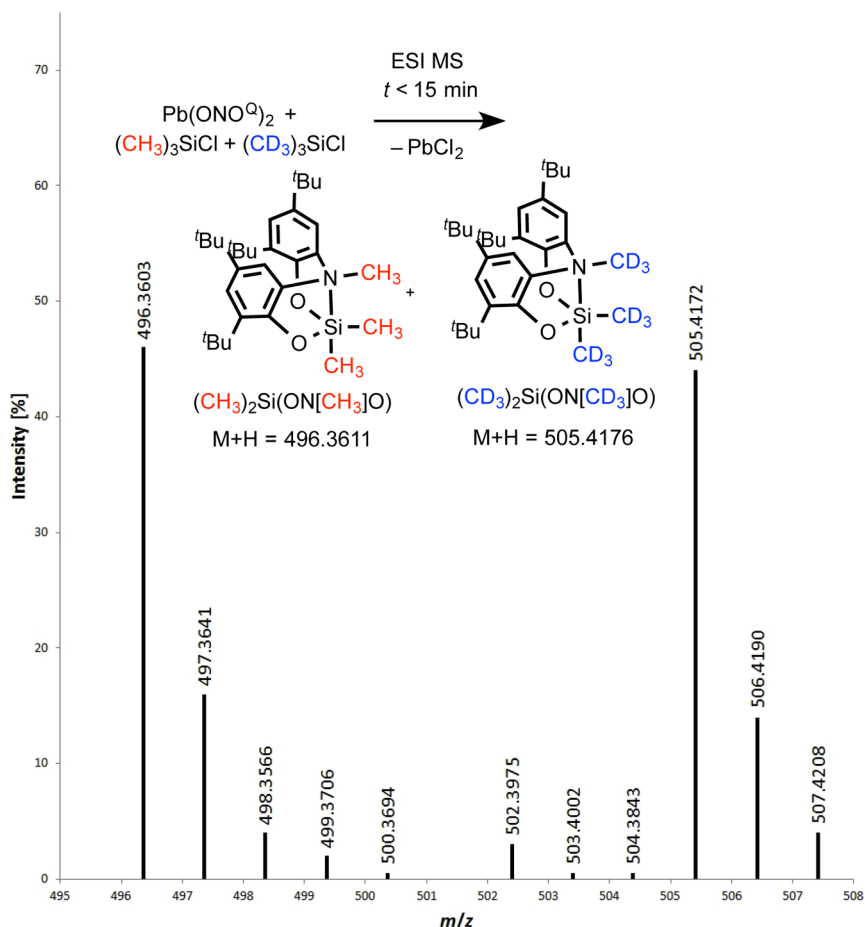
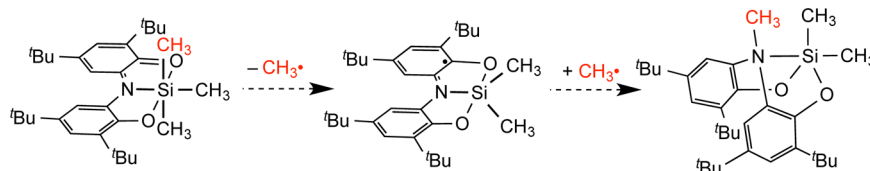


**Special Issue:** Mechanisms in Metal-Based Organic Chemistry

**Received:** August 15, 2014

**Published:** October 7, 2014



Scheme 2. Possible Homolytic Pathway for Silicon-to-Nitrogen Migration in  $\text{Me}_3\text{Si}(\text{ONO}^\text{Q})$ Figure 1. ESI mass spectrum of reaction mixture  $(\text{CH}_3)_3\text{SiCl}/(\text{CD}_3)_3\text{SiCl}$  with  $\text{Pb}(\text{ONO}^\text{Q})_2$  ( $\text{CHCl}_3$ , 60 °C, 15 min).

rather ordinary aryloxysilane seems unlikely, but the presence of nearby donor atoms allows for the possibility of chelation to form octahedral  $\kappa^3\text{-R}(\text{X})(\text{Y})\text{Si}(\text{ONO}^\text{Q})$  (analogous tin compounds are isolable with  $\text{X} = \text{Y} = \text{Cl}$ ).<sup>6</sup> Evidently, this hypervalent silane is primed for unusually facile carbon–silicon bond scission, resulting ultimately in net migration of the alkyl or aryl group to nitrogen, reduction of the iminoquinone, and formation of pentacoordinate  $(\text{X})(\text{Y})\text{Si}(\text{ON}[\text{R}]\text{O})$ . This reaction provides a system where hypervalency is achieved by chelation rather than the addition of external nucleophiles and thus offers the possibility of investigating the details of the carbon–nitrogen bond-forming step in an unusually well-defined complex. Those details are explored here.

## RESULTS AND DISCUSSION

**Establishing the Intramolecularity of Silicon-to-Nitrogen Methyl-Group Migration.** Silylation of the oxidized ligand in  $\text{Pb}(\text{ONO}^\text{Q})_2$  with chlorosilanes leads to the precipitation of lead chloride and net migration of a methyl or phenyl group from silicon to nitrogen. The reduced

$\text{ON}[\text{R}]\text{O}$  ligand is coordinated in a tridentate fashion to the silicon resulting in a trigonal bipyramidal product (Scheme 1).<sup>5</sup>

One possible pathway for this migration would be the homolytic scission of the carbon–silicon bond followed by capture of the carbon radical by the nitrogen atom (Scheme 2). Although silicon–carbon bonds are normally too strong for this to be a viable pathway under such mild conditions,<sup>7</sup> this may be an exceptional case due to the associated redox chemistry of the  $\text{ONO}^\text{Q}$  ligand. This silicon-containing radical would be ligand centered, and  $(\text{ONO}^\text{SQ})\text{SiMe}_2$ ,<sup>5</sup> as well as analogous diorganogermanium,<sup>8</sup> -tin,<sup>6,9,10</sup> and -lead<sup>11</sup> radicals, is isolable. Indeed, production of  $(\text{ONO}^\text{SQ})\text{SiMe}_2$  from the reaction of  $\text{HONO}^\text{Q}$  and  $\text{Me}_3\text{SiCl}$  has been documented on the basis of EPR data,<sup>10</sup> and the development of intense purple colors during the reactions of chlorosilanes with  $\text{Pb}(\text{ONO}^\text{Q})_2$  is also consistent with the presence of these radicals during the migration reaction. Capture of even highly reactive radicals such as methyl by persistent radicals can be highly efficient.<sup>12</sup>

To probe the possible role of homolytic pathways in this reaction, a crossover experiment involving the reaction of an

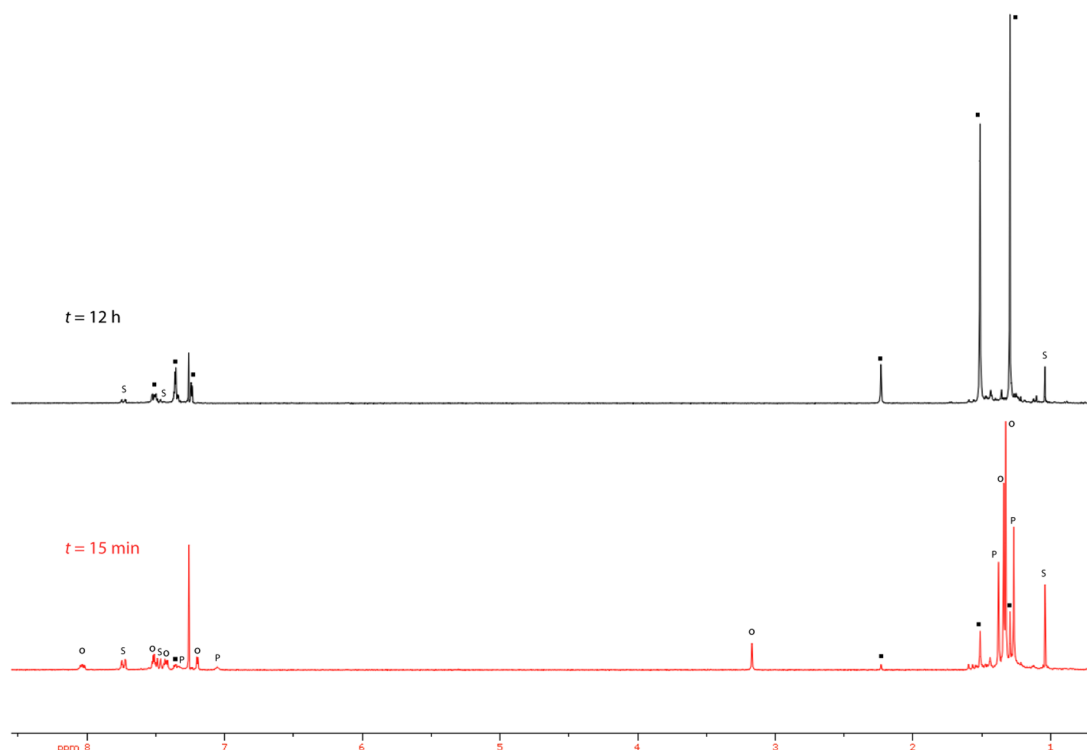
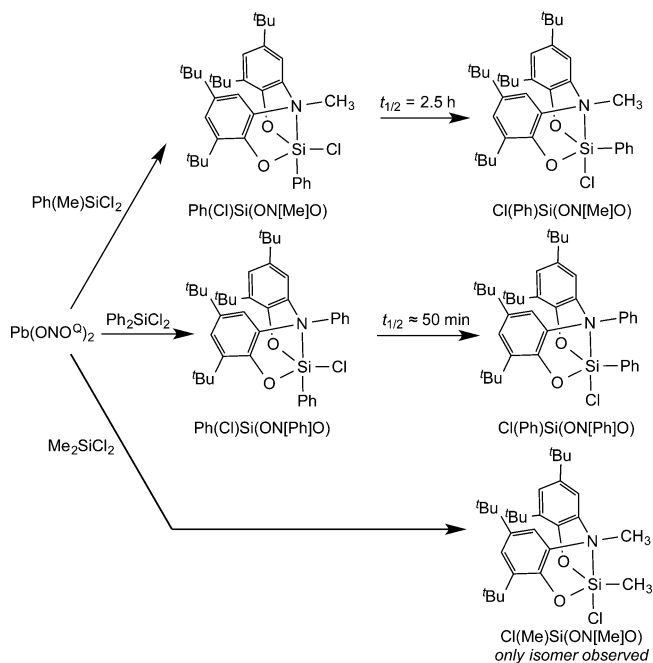


**Figure 2.** In situ  $^1\text{H}$  NMR spectra ( $\text{CDCl}_3$ , 300 MHz) of the reaction of  $\text{Pb}(\text{ONO}^\text{Q})_2$  with  $\text{Ph}(\text{Me})\text{SiCl}_2$ . Bottom:  $t = 15$  min. Top:  $t = 12$  h. Key:  $\circ = \text{Ph}(\text{Cl})\text{Si}(\text{ON}[\text{Me}]\text{O})$  (kinetic isomer).  $\blacksquare = \text{Cl}(\text{Ph})\text{Si}(\text{ON}[\text{Me}]\text{O})$  (thermodynamic isomer).  $\text{S} = \text{Ph}(\text{Me})\text{SiCl}_2$ .  $\text{P} = \{\text{PbCl}(\text{ONO}^\text{Q})\}_n$ .

equimolar mixture of  $(\text{CH}_3)_3\text{SiCl}$  and  $(\text{CD}_3)_3\text{SiCl}$  with  $\text{Pb}(\text{ONO}^\text{Q})_2$  was undertaken. Electrospray mass spectrometry of the reaction mixture after 15 min (Figure 1) shows a clear preponderance of the  $d^0$ - and  $d^9$ -isotopomers  $(\text{CH}_3)_2\text{Si}(\text{ON}[\text{CH}_3]\text{O})$  ( $m/z = 496.3068$ ,  $M + \text{H}$  calcd 496.3611) and  $(\text{CD}_3)_2\text{Si}(\text{ON}[\text{CD}_3]\text{O})$  ( $m/z = 505.4172$ ,  $M + \text{H}$  calcd 505.4176). There is a detectable amount of the mixed ( $d^3$  and  $d^6$ ) isotopomers, but they account for less than 5% of the signal intensity. This amount does not change after incubation for up to 48 h at room temperature; thus, any crossover does not appear to be due to the exchange of the  $\text{ON}[\text{Me}]\text{O}^{2-}$  ligand between  $\text{Me}_2\text{Si}^{2+}$  fragments after migration. Thus, the reaction is predominantly intramolecular. Even if some of the  $(\text{ONO}^\text{SQ})\text{SiMe}_2$  radical is formed, it does not appear to intervene significantly in the pathway toward the migrated product  $\text{Me}_2\text{Si}(\text{ON}[\text{Me}]\text{O})$ .

**Stereoselectivity of Migration Reactions.** Phenyl-(methyl)dichlorosilane reacts with  $\text{Pb}(\text{ONO}^\text{Q})_2$  to give the product  $\text{Cl}(\text{Ph})\text{Si}(\text{ON}[\text{Me}]\text{O})$  with exclusive migration of the methyl, rather than the phenyl, group. The stereochemistry of the isolated product, determined by crystallography, has the chloro group axial in the trigonal bipyramid, opposite nitrogen.<sup>5</sup> This is consistent with the well-known preference of electronegative substituents to occupy apical positions in hypervalent compounds, based on the more ionic character of these bonds.<sup>13</sup> In situ monitoring of the reaction (Figure 2) reveals a kinetic product of migration,  $\text{Ph}(\text{Cl})\text{Si}(\text{ON}[\text{Me}]\text{O})$ , assigned as the stereoisomer with apical phenyl and equatorial chloride groups (Scheme 3). The *N*-methyl peak at 3.17 ppm in the  $^1\text{H}$  NMR spectrum clearly indicates that migration has taken place. The chemical shift is similar to that of  $\text{NCH}_3$  in  $\text{Me}_2\text{Si}(\text{ON}[\text{CH}_3]\text{O})$  (2.98 ppm) or  $\text{Cl}(\text{Me})\text{Si}(\text{ON}[\text{CH}_3]\text{O})$  (3.02 ppm), but downfield of the peak in the thermodynamic product  $\text{Cl}(\text{Ph})\text{Si}(\text{ON}[\text{CH}_3]\text{O})$  (2.23 ppm) where the placement of the

**Scheme 3. Stereoselectivity of Migration in Reactions of  $\text{R}_1\text{R}_2\text{SiCl}_2$  with  $\text{Pb}(\text{ONO}^\text{Q})_2$  ( $\text{R}_1, \text{R}_2 = \text{Me, Ph; Ph, Ph; or Me, Me}$ )**

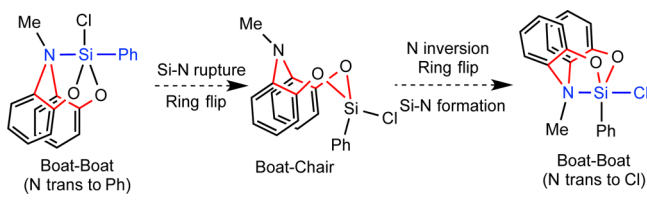


*N*-methyl group in the shielding cone of the phenyl group results in a substantial upfield shift. Only traces of the thermodynamic product are present at very early times in the reaction (kinetic stereoselectivity > 6:1).

The kinetic product isomerizes to the thermodynamic product  $\text{Cl}(\text{Ph})\text{Si}(\text{ON}[\text{Me}]\text{O})$  over the course of approximately 12 h in chlorinated solvents ( $k_{\text{isom}} = 8.0(11) \times 10^{-5} \text{ s}^{-1}$

in  $\text{CD}_2\text{Cl}_2$  at 21 °C,  $\Delta G^\circ = 22.7(2) \text{ kcal mol}^{-1}$ , Figure S2 in the Supporting Information (SI)). A plausible mechanism for this isomerization is shown in Scheme 4. As previously discussed,<sup>5</sup>

**Scheme 4. Stereoisomerization Mechanism of  $\text{Ph}(\text{Cl})\text{Si}(\text{ON}[\text{Me}]\text{O})$  (*tert*-Butyl Groups Omitted for Clarity)**



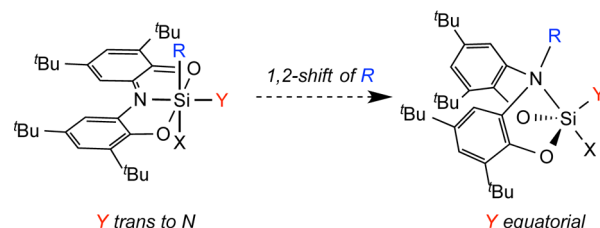
the bicyclic nature of the dioxoazasilocene ring, and the presence of a substituent on the nitrogen, renders the two faces of the chelate inequivalent and prevents Berry pseudorotations. A turnstile rotation is theoretically possible, but a ring-inversion mechanism is more consistent with the data. In particular, the barrier to isomerization in this structure is substantially greater than that of dibenzodioxasilocene  $\text{CH}_2[\text{C}_6\text{H}_2-3,5\text{-}^t\text{Bu}_2-2\text{-O}]_2\text{SiMe}_2$  ( $\Delta G^\circ = 13.9 \text{ kcal mol}^{-1}$ ),<sup>14</sup> which lacks the Si–N bond. The difference is in agreement with observations of diethanolamine complexes  $\text{R}(\text{R}')\text{Si}([\text{OCH}_2\text{CH}_2]_2\text{NMe})$  ( $\Delta G^\circ = 9\text{--}13 \text{ kcal mol}^{-1}$ ), where the barrier is likely dominated by the thermodynamics of amine dissociation.<sup>15</sup> Similarly, breaking the Si–N bond in pentacoordinate fluorosilanes with intramolecularly coordinated dimethylamino groups requires 10–12  $\text{kcal mol}^{-1}$ .<sup>16</sup> The importance of Si–N bond breaking is also reflected in the higher barriers exhibited by the compounds discussed here than in  $\text{Me}(\text{Ph})\text{Si}(\text{ON}[\text{Me}]\text{O})$ , which contains a chlorine-free silicon that is less Lewis acidic.<sup>5</sup>

The reaction of  $\text{Ph}_2\text{SiCl}_2$  with  $\text{Pb}(\text{ONO}^\text{Q})_2$  follows a similar course, with kinetic stereoisomer  $\text{Ph}(\text{Cl})\text{Si}(\text{ON}[\text{Ph}]\text{O})$  observed selectively (>5:1) at early reaction times and then isomerizing to the thermodynamic isomer  $\text{Cl}(\text{Ph})\text{Si}(\text{ON}[\text{Ph}]\text{O})$  (Figure S2 in the SI). The stereochemistry of the thermodynamic product has been confirmed by X-ray crystallography (Tables S1 and S2 and Figure S1 in the SI) with the chlorine axial and the phenyl equatorial. The Si–NPh bond (2.7146(12) Å) is longer than the Si–NMe bond in  $\text{Cl}(\text{Ph})\text{Si}(\text{ON}[\text{Me}]\text{O})$  (2.3043(16) Å), which is consistent with previously observed structural effects of decreased Lewis basicity of the NPh compared to the NMe group.<sup>5</sup> This decrease in basicity also leads to more facile dissociation of nitrogen from silicon, as judged by the greater rate of isomerization of the kinetic product  $\text{Ph}(\text{Cl})\text{Si}(\text{ON}[\text{Ph}]\text{O})$  ( $t_{1/2} \approx 50 \text{ min}$ ).

The analogous reaction with  $\text{Me}_2\text{SiCl}_2$  proceeds differently, with only the thermodynamic stereoisomer  $\text{Cl}(\text{Me})\text{Si}(\text{ON}[\text{Me}]\text{O})$  observed within 5 min at room temperature. Even reactions carried out at –30 °C (at which temperature silylation is complete in ~80 min) produce only this isomer. In principle, this may be due to rapid isomerization of a kinetically formed stereoisomer, but the trends observed in the rates of isomerization of  $\text{Ph}(\text{Cl})\text{Si}(\text{ON}[\text{Ph}]\text{O})$  and  $\text{Ph}(\text{Cl})\text{Si}(\text{ON}[\text{Me}]\text{O})$  suggest that, if anything, the putative isomer  $\text{Me}(\text{Cl})\text{Si}(\text{ON}[\text{Me}]\text{O})$  would isomerize the most slowly of the three and would certainly be observable. We thus conclude that  $\text{Cl}(\text{Me})\text{Si}(\text{ON}[\text{Me}]\text{O})$  is both kinetically and thermodynamically favored in the reaction.

The stereoselectivity of the reaction has clear mechanistic implications. If migration is intramolecular, then the migrating group must occupy a position cis to nitrogen in the octahedral  $\kappa^3$  intermediate, and the group that is trans to nitrogen prior to migration must occupy an equatorial position in the trigonal bipyramidal product after migration (Scheme 5). Thus,

**Scheme 5. Stereochemical Course of Migration of  $\kappa^3\text{-R}(\text{X})(\text{Y})\text{Si}(\text{ONO}^\text{Q})$**



$\text{Ph}(\text{Me})(\text{Cl})\text{Si}(\text{ONO}^\text{Q})$  and  $\text{Ph}_2(\text{Cl})\text{Si}(\text{ONO}^\text{Q})$  must both undergo migration predominantly from the isomer in which both carbon substituents are mutually trans, whereas  $\text{Me}_2(\text{Cl})\text{Si}(\text{ONO}^\text{Q})$  undergoes migration from the isomer in which one of the methyl groups is trans to nitrogen. This implies that the exclusive methyl migration observed in  $\text{Ph}(\text{Me})(\text{Cl})\text{Si}(\text{ONO}^\text{Q})$  is due to its migratory aptitude being intrinsically greater than that of phenyl because both are stereochemically competent to migrate in the reactive isomer of the intermediate.

**DFT Analysis of the Migration Mechanism.** The stereoselectivity of the migration has two possible origins. The formation of the octahedral  $\kappa^3$  intermediate might be rate-limiting, in which case migration would occur faster than the octahedral isomer could isomerize. In this scenario, the product formed would be determined by which  $\kappa^3$  isomer formed the fastest. Alternatively, if  $\kappa^1$  and  $\kappa^3$  isomers can interconvert before migration, the preferred product would be formed via the isomer that has the lowest-energy transition state for migration.

To gain further insight into this issue, we explored the reaction mechanism through DFT calculations. The reaction of  $\text{Ph}(\text{Me})(\text{Cl})\text{Si}(\text{ONO}^\text{Q})$  is of particular interest because it affords the opportunity to explore both the stereo- and chemoselectivity of the migration reaction (Figure 3). Calculations were carried out using the B3LYP functional, which has been found to perform satisfactorily in describing hypervalent silicon species.<sup>17</sup> A 6-31G\* basis set was used for all atoms using a simplified ONO ligand in which the *tert*-butyl groups were replaced with hydrogens. Energies and geometries are reported for calculations using a continuum solvation model, but gas-phase calculations give qualitatively similar results. Three separate transition states were found for the ring closure to form  $\kappa^3$  isomers ( $\kappa^1\text{-TS-}\kappa^3$ ) corresponding to the three distinct octahedral complexes  $\kappa^3\text{-R}(\text{X})(\text{Y})\text{Si}(\text{ONO}^\text{Q})$  (X trans to R, Y trans to N), which were all identified as energy minima. (Tetrahedral conformers are expected to be able to interconvert by crossing small energetic barriers by rotation about the silicon–oxygen bond, and no attempt was made to identify individual conformers of the  $\kappa^1$  compound.) A 1,2-alkyl or -aryl migration from octahedral silicon to nitrogen leads to the formation of pentacoordinate products  $(\text{X})(\text{Y})\text{Si}(\text{ON}[\text{R}]\text{O})$ . Four distinct transition states for migration were identified. In the isomer of the  $\kappa^3$  compound with methyl trans to N (1- $\kappa^3$ ), only phenyl can migrate, while only methyl can migrate if

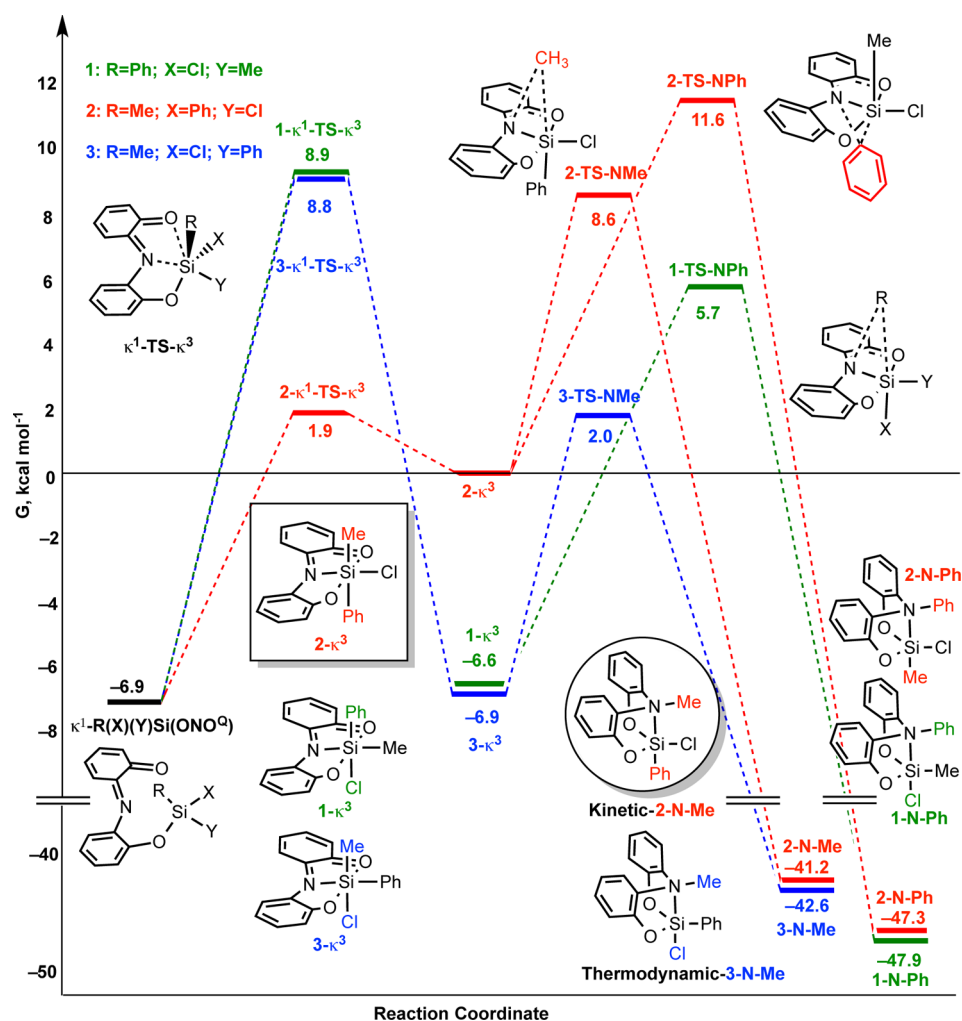


**Figure 3.** Computed reaction coordinate of  $\text{Ph}(\text{Me})(\text{Cl})\text{Si}(\text{ONO}^Q)$  (B3LYP, 6-31G\*). Calculations refer to the ONO ligand in which *tert*-butyl groups have been replaced with H. The pathway that is observed experimentally to predominate, via the boxed intermediate  $2\text{-}\kappa^3$  through the circled kinetic product  $2\text{-N-Me}$ , is shown in red.

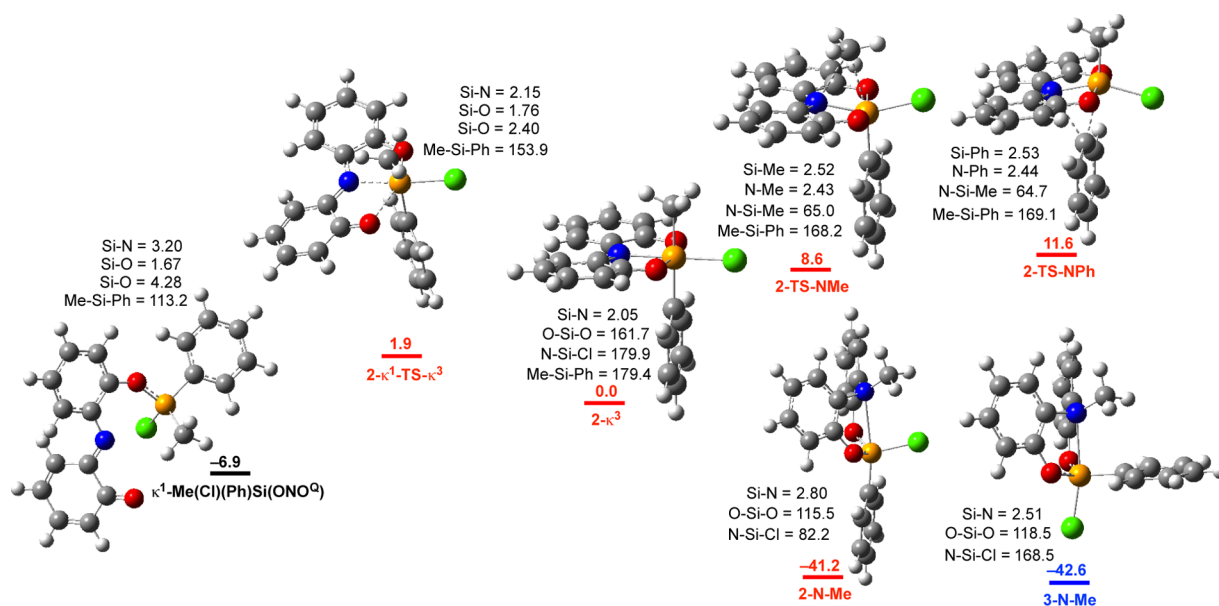


**Figure 4.** Calculated geometries (bond distance = Å, bond angle = deg) and energies ( $\text{kcal mol}^{-1}$ ) of intermediates, transition states, and products in the major reaction coordinate of  $\text{Ph}(\text{Cl})(\text{Me})\text{Si}(\text{ONO}^Q)$ .



phenyl is trans to N ( $3-\kappa^3$ ). In the isomer with Cl trans to N ( $2-\kappa^3$ ), transition states for both phenyl and methyl migration could be found. Each of these transition states leads to a distinct isomer of the migrated product, differing in which group migrates (Me or Ph) and is axial in the trigonal bipyramidal product (Cl or R). The interconversion of these stereoisomers was not explored computationally. Similar computational analyses of the reactions of  $\text{Me}_3\text{Si}$ -,  $\text{Ph}_2(\text{Cl})\text{Si}$ -, and  $\text{Me}_2(\text{Cl})\text{Si}(\text{ONO}^\text{Q})$  were also carried out (see SI for details).

In all cases, intramolecular migration of a methyl or phenyl group from the  $\kappa^3$  isomer of  $\text{R}_3\text{Si}(\text{ONO}^\text{Q})$  is a facile process, with calculated barriers ranging from 2.0 to 12.8 kcal mol<sup>-1</sup>. Although both methyl and phenyl migration are feasible, methyl migration is calculated to be kinetically preferred over phenyl migration. The clearest comparison is migration from  $2-\kappa^3$ , in which both groups are stereochemically poised to migrate, and in which methyl migration is preferred over phenyl migration by 3.0 kcal mol<sup>-1</sup>. Similar results are obtained even in comparisons between analogues, such as  $1-\kappa^3$  and  $3-\kappa^3$ , where the barrier to phenyl migration in the former is 3.4 kcal mol<sup>-1</sup> higher than that of methyl migration in the latter. This is in excellent agreement with the experimental observation that methyl migration is observed exclusively (>20:1 over phenyl) when both are possible.

Calculations show a strong kinetic preference for forming the  $\kappa^3$  isomer with equatorial chlorine. Typically, the  $\kappa^1\text{-TS-}\kappa^3$  transition state to form this isomer is 6–8 kcal mol<sup>-1</sup> lower in energy than the transition states to form the isomers with methyl or phenyl equatorial. The chelation reaction can be viewed as a nucleophilic attack of the nitrogen on silicon (Figure 4), and the trajectory that positions the nitrogen anti to the chlorine maximizes its interaction with the Si–Cl  $\sigma^*$  orbital and stabilizes the transition state. Although this isomer is the fastest to form, it is calculated to be the least stable thermodynamically, typically by about 6 kcal mol<sup>-1</sup>. As expected, the thermodynamically preferred six-coordinate isomers have the two hydrocarbyl groups trans to more electronegative substituents (N and Cl), maximizing bonding in the hypervalent species.

Surprisingly, the difference in stability of the octahedral  $\kappa^3$  isomers does not translate to a difference in reactivity. The barriers to phenyl migration from  $1-\kappa^3$  and  $2-\kappa^3$  differ by 0.7 kcal mol<sup>-1</sup>, and the barriers to methyl migration from  $2-\kappa^3$  and  $3-\kappa^3$  differ by only 0.3 kcal mol<sup>-1</sup>. The differences in the absolute energies of the migration transition states are dominated by the relative energies of the  $\kappa^3$  intermediates.

These calculations therefore lend strong support for the hypothesis that the observed preference of  $\text{Ph}(\text{Me})(\text{Cl})\text{Si}(\text{ONO}^\text{Q})$  and  $\text{Ph}_2(\text{Cl})\text{Si}(\text{ONO}^\text{Q})$  to react via the chlorine-equatorial isomer (e.g.,  $2-\kappa^3$ ) must arise from this isomer's preferential and effectively irreversible formation rather than from its enhanced propensity for migration. The calculated difference in barrier heights between (methyl) migration from  $2-\kappa^3$  ( $2\text{-TS-NMe}$ ) and its conversion to  $3-\kappa^3$  ( $3\text{-}\kappa^1\text{-TS-}\kappa^3$ ) is small (0.2 kcal mol<sup>-1</sup>), suggesting that small changes in the substrate could shift the rate-limiting step from chelation to migration, which would result in kinetic, as well as thermodynamic, formation of the trigonal bipyramidal product with axial chlorine. This is precisely what is observed experimentally with  $\text{Me}_2(\text{Cl})\text{Si}(\text{ONO}^\text{Q})$ . This changeover is plausible; substitution reactions are often faster in methyl- rather than in phenylsilanes,<sup>18</sup> leading to the possibility of faster

$\kappa^1\text{--}\kappa^3$  equilibration. Computationally, the difference in calculated barriers between isomerization and migration remains small.

In all cases, migration is highly exoergic ( $\Delta G^\circ < -30$  kcal mol<sup>-1</sup> for formation of migrated products from  $\kappa^1$  silanes). The calculations generally predict that the five-coordinate product with axial chlorine is more stable than that with axial methyl or phenyl, but the energy differences are small (0–1 kcal mol<sup>-1</sup>) compared to those from the experiment in which only axial chlorine is observed at equilibrium (>30:1 by NMR,  $\Delta G^\circ > 2$  kcal mol<sup>-1</sup>).

#### The Nature and Selectivity of the Migration Reaction.

As the migration reaction takes place, the ONO ligand is formally reduced, and the silicon atom is formally oxidized. The redox activity of the ONO ligand originates from the  $\pi$  orbital that is a combination of in-phase p orbitals on each of its ligating ONO atoms (of  $B_2$  symmetry in the  $C_{2v}$  point group, Figure 5b). This orbital is raised in energy due to the

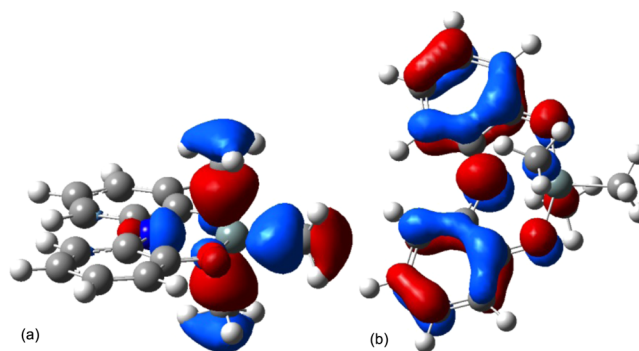


**Figure 5.** Frontier orbitals of  $\kappa^3\text{-Me}_3\text{Si}(\text{ONO}^\text{Q})$ . (a) HOMO ( $A_1$  symmetry) centered on a carbon nucleophile. (b) LUMO ( $B_2$  symmetry) centered on the ONO ligand.

antibonding interaction of these p lone pairs with filled  $\pi$ -bonding orbitals of the benzene rings.<sup>19</sup> The source of the electrons for reducing the ONO ligand is the in-phase combination of  $\sigma$  orbitals, which is the nonbonding component of the 3-center, 4-electron-bond characteristic of hypervalent main-group compounds (Figure 5a).<sup>20</sup> The migration is well described as a nucleophilic 1,2-shift.<sup>21</sup>

In familiar cases of nucleophilic 1,2-migrations to electron-deficient carbon centers, the ability of a migrating phenyl group to delocalize the charge at the migration terminus can stabilize the transition state and accelerate migration.<sup>22</sup> Among thermal 1,2-shifts from silicon, the relative migratory aptitudes of phenyl and methyl vary,<sup>23</sup> but the migrations described here are to our knowledge unique in displaying complete selectivity of methyl over phenyl. The origin of this selectivity is not entirely clear. Geometrically, the plane of the phenyl group is computed to be roughly perpendicular to the Si–N bond both in the  $\kappa^3$  intermediate and in the migration transition state (Figure 4); thus, there is no geometric impediment to charge delocalization. However, these silicon-to-nitrogen shifts are rather different electronically from more familiar 1,2-shifts such as those in carbocations. In a Wagner–Meerwein shift, the migration terminus is an empty carbon p orbital, which is highly reactive. The electrons principally involved in the migration are carbon–carbon  $\sigma$ -bonding electrons, which are extremely low in energy. Thus, the availability of higher-lying orbitals, such as the  $\pi$ -bonding orbitals of the phenyl group that

can interact with and stabilize the carbocation, can play an important role in facilitating migration. In contrast, the empty orbital on the  $\text{ONO}^\ominus$  fragment is not extremely low-lying due to its antibonding character. Indeed, many compounds of  $\text{ONO}^\ominus$  (such as the reactant  $\text{Pb}(\text{ONO}^\ominus)_2$ ) are isolable and relatively unreactive. Furthermore, the electrons involved in the migration are not  $\sigma$  bonding, but rather are  $\sigma$  nonbonding, in these hypervalent silicon compounds, and thus significantly higher in energy. The ability of the aryl group to donate  $\pi$  electrons is thus much less important in light of the lower electron demand of the migration terminus and the higher energy of the donor orbital. The unimportance of electron delocalization into the phenyl  $\pi$  system is corroborated computationally by the lack of elongation of the phenyl C1–C2 and C1–C6 bonds in the transition state. In fact, these bonds actually contract slightly in the transition state (1.385 Å vs 1.410 Å in the reactants), in contrast to the lengthening calculated for aryl-bridged carbocations (to 1.442 Å).<sup>24</sup>

Because the phenyl  $\pi$  system is not important in migration, other factors that favor methyl migration can rise to the fore. The  $\text{sp}^3$ -hybridized methyl group would be expected both to be more nucleophilic and to form a weaker bond to silicon than the  $\text{sp}^2$ -hybridized phenyl group, and both of these factors should favor migration of the methyl group. If this unusual selectivity is indeed the result of the combination of hypervalency and low electron demand of the migration terminus, it may well have implications for the class of reactions in which nucleophiles induce alkyl or aryl transfer from silicon. Under the appropriate conditions, alkyl transfers may become competitive with or even faster than transfer of aryl or alkenyl groups.

## CONCLUSIONS

Methyl and phenyl migrations in silylated aryloxyiminoquinones occur via initial formation of a  $\kappa^1$ -aryloxyasilane, which then chelates the remaining donor atoms to form a six-coordinate  $\kappa^3$  complex. Migration takes place from this hypervalent intermediate by a facile 1,2-shift, as shown experimentally by the lack of crossover and computationally by the observation of low-energy transition states for intramolecular migration. The stereochemistry of the product formed is a marker for the stereochemistry of the reactive octahedral intermediate, as the group trans to N in the octahedral  $\kappa^3$ - $\text{ONO}^\ominus$  intermediate becomes equatorial in the kinetically formed product, and stereoisomerization of the five-coordinate products is slow when one of the groups on silicon is chlorine. The observation of the preponderant formation of the counterthermodynamic product from  $\text{Ph}(\text{Me})(\text{Cl})\text{Si}(\text{ONO}^\ominus)$  and  $\text{Ph}_2(\text{Cl})\text{Si}(\text{ONO}^\ominus)$ , but not from  $\text{Me}_2(\text{Cl})\text{Si}(\text{ONO}^\ominus)$ , is best explained by the similarity in barrier heights for isomerization of the octahedral intermediate and for migration. In the former two compounds, formation of the octahedral intermediate is rate-determining whereas in the latter it can stereoisomerize, and migration takes place from the thermodynamically favored isomer of  $\text{Me}_2\text{ClSi}(\text{ONO}^\ominus)$ . DFT calculations reproduce the unusual experimental observation that methyl has a migratory aptitude greater than that of phenyl in these nucleophilic 1,2-shifts. This selectivity is attributed to the low electron deficiency of the migration terminus and the relatively high electron density of the migration source, which is the  $\sigma$ -nonbonding combination of the hypervalent silane.

## EXPERIMENTAL SECTION

All procedures were carried out under an inert atmosphere in a nitrogen-filled glovebox or on a vacuum line. Solvents were dried over 4 Å molecular sieves followed by  $\text{CaH}_2$ .  $\text{Pb}(\text{ONO}^\ominus)_2$  was prepared as described<sup>5,25</sup> by self-assembly from ammonia, 3,5-di-*tert*-butylcatechol, 3,5-di-*tert*-butyl-1,2-benzoquinone, and  $\text{PbF}_2$ . Chlorosilanes were purchased from Aldrich (except  $(\text{CD}_3)_3\text{SiCl}$ , which was purchased from CDN Isotopes) and were stored and dispensed in an inert-atmosphere glovebox. Samples for ESI mass spectrometry were injected as acetonitrile solutions, preceded and followed by methanol.

**Crossover Experiment with Protio and Deutero Chlorotrimethylsilane.** 2,4,8,10-Tetra-*tert*-butyl-6,6,12-trimethyl-12*H*-dibenzo[d,g][1,3,6,2]dioxazasilocine,  $\text{Me}_2\text{Si}(\text{ON}[\text{Me}]\text{O})$ , is generated in situ with reaction times of less than 5 min at ambient temperatures. For the crossover experiment, equal amounts of  $(\text{CH}_3)_3\text{SiCl}$  (7  $\mu\text{L}$ , 0.055 mmol) and its deutero analog,  $(\text{CD}_3)_3\text{SiCl}$  (7.2  $\mu\text{L}$ , 0.057 mmol) were mixed in 0.5 mL of  $\text{CHCl}_3$  and syringed into 1 mL  $\text{Pb}(\text{ONO}^\ominus)_2$  (30.2 mg, 0.028 mmol) in  $\text{CDCl}_3$  at 60 °C. The reaction solution was allowed to cool to room temperature and analyzed after 15 min, 4 h, and 48 h by electrospray mass spectrometry. No significant changes were observed in the spectra over this time period.

**2,4,8,10-Tetra-*tert*-butyl-6-chloro-12-methyl-6-phenyl-12*H*-dibenzo[d,g][1,3,6,2]dioxazasilocine,  $\text{Ph}(\text{Cl})\text{Si}(\text{ON}[\text{Me}]\text{O})$ , Kinetic Isomer.** In an NMR tube sealed with a septum cap, 0.0105 g of  $\text{Pb}(\text{ONO}^\ominus)_2$  (0.0100 mmol) was dissolved in 600  $\mu\text{L}$  of  $\text{CDCl}_3$ . Dichloro(methyl)phenylsilane (4.0  $\mu\text{L}$ , 0.24 mmol, 1.2 equiv) was added by syringe through the septum, and a  $^1\text{H}$  NMR spectrum was recorded within 15 min.  $^1\text{H}$  NMR:  $\delta$  1.33, 1.34 (s, 18H each), 3.17 (s, 3H), 7.20 (d,  $J$  = 2 Hz, 2H), 7.42 (m, 3H), 7.51 (d,  $J$  = 2 Hz, 2H), 8.03 (m, 2H).

**2,4,8,10-Tetra-*tert*-butyl-6-chloro-6,12-diphenyl-1*H*-dibenzo[d,g][1,3,6,2]dioxazasilocine,  $\text{Ph}(\text{Cl})\text{Si}(\text{ON}[\text{Ph}]\text{O})$ , Kinetic Isomer.** In an NMR tube sealed with a septum cap, 0.0099 g of  $\text{Pb}(\text{ONO}^\ominus)_2$  (0.0094 mmol) was dissolved in 600  $\mu\text{L}$  of  $\text{CDCl}_3$ . Diphenyldichlorosilane (6.5  $\mu\text{L}$ , 0.031 mmol, 1.6 equiv) was added by syringe through the septum, and a  $^1\text{H}$  NMR spectrum was recorded within 20 min.  $^1\text{H}$  NMR:  $\delta$  1.28, 1.33 (s, 18H each), 6.54 (d,  $J$  = 8 Hz, 2H), 6.90 (t,  $J$  = 8 Hz, 1H), 7.17 (t,  $J$  = 8 Hz, 2H), 7.29 (d,  $J$  = 2 Hz, 2H), 7.38 (d,  $J$  = 2 Hz, 2H), 7.42 (t,  $J$  = 8 Hz, 1H), 7.45 (t,  $J$  = 8 Hz, 2H), 7.94 (d,  $J$  = 8 Hz, 2H).

**Attempted Observation of Kinetic Isomer 2,4,8,10-Tetra-*tert*-butyl-6-chloro-6,12-dimethyl-12*H*-dibenzo[d,g][1,3,6,2]dioxazasilocine,  $\text{Cl}(\text{Me})\text{Si}(\text{ON}[\text{Me}]\text{O})$ .** Dichlorodimethylsilane (5.0  $\mu\text{L}$ , 0.040 mmol) was injected into a 600  $\mu\text{L}$  of  $\text{CD}_2\text{Cl}_2$  solution of  $\text{Pb}(\text{ONO}^\ominus)_2$  (0.0203 g, 0.020 mmol) at –78 °C. The sample was inserted into a precooled probe of an NMR spectrometer, and  $^1\text{H}$  NMR spectra were first recorded at –50 °C. Only a single product of migration, the isomer  $\text{Cl}(\text{Me})\text{Si}(\text{ON}[\text{Me}]\text{O})$ , that has been previously reported<sup>5</sup> first appears at –40 °C as silylation of the  $\text{ONO}^\ominus$  ligand commences. Silylation is complete in approximately 80 min at –30 °C. At room temperature, the same migration reaction is complete within 5 min as judged by  $^1\text{H}$  NMR, and only this same isomer is observed.

**Measurement of  $k_{\text{isom}}$  for Conversion of  $\text{Ph}(\text{Cl})\text{Si}(\text{ON}[\text{Me}]\text{O})$  to  $\text{Cl}(\text{Ph})\text{Si}(\text{ON}[\text{Me}]\text{O})$ .** A solution of  $\text{Pb}(\text{ONO}^\ominus)_2$  (12.7 mg, 0.012 mmol) dissolved in 600  $\mu\text{L}$   $\text{CD}_2\text{Cl}_2$  containing dimethylterephthalate as an internal standard was placed in a screw-cap NMR tube with a septum cap. A 2-fold excess of  $\text{Ph}(\text{Me})\text{SiCl}_2$  (8  $\mu\text{L}$ , 0.049 mmol) dissolved in 25  $\mu\text{L}$  of  $\text{CD}_2\text{Cl}_2$  was injected through the septum cap. After vigorous mixing of the NMR tube for 30 s, the tube was inserted into the probe of the spectrometer, and  $^1\text{H}$  NMR spectra were collected at 8 min intervals for 10 h. Concentration data for the kinetic and thermodynamic products over the time course of the isomerization were determined from normalized integrals of the *N*-methyl group at 3.17 and 2.23 ppm, respectively. The concentration versus time data were fit to an exponential decay curve using the program Kaleidagraph (Synergy Software, v. 4.1) to give a first-order rate constant of isomerization.

**X-ray Crystallography.** Crystals of  $\text{Cl}(\text{Ph})\text{Si}(\text{ON}[\text{Ph}]\text{O})$  were grown by layering a concentrated solution of the complex in  $\text{CHCl}_3$  with acetonitrile. The crystals were placed in inert oil before being

transferred to the cold N<sub>2</sub> stream of the diffractometer. Data were reduced and corrected for absorption using the program SADABS. The structure was solved using direct methods. All non-hydrogen atoms not apparent from the initial solutions were found on difference Fourier maps, and all heavy atoms were refined anisotropically.

The *tert*-butyl group centered on C28 in (Cl)(Ph)Si(ON[Ph]O) was disordered in two different orientations. The disordered *tert*-butyl group was modeled by constraining the thermal parameters of the methyl carbons to be equal to those of the carbons opposite them in the other orientation. The occupancy of the major orientation refined to 69.1(2)%. Hydrogens on the disordered methyl groups were placed in calculated positions, while all other hydrogen atoms were found on the difference Fourier map and refined isotropically. Calculations used SHELXTL (Bruker AXS),<sup>26</sup> with scattering factors and anomalous dispersion terms taken from the literature.<sup>27</sup> Further details about the structure are given in Table S1 of the SI.

**Computational Methods.** Geometry optimizations were performed on all complexes using a 6-31G\* basis set and a B3LYP functional using the Gaussian09 suite of programs.<sup>28</sup> A PCM solvation model using the dielectric constant of dichloromethane was applied, except for structures in the reaction coordinate that leads to Me<sub>2</sub>Si(ON[Me]O), which were conducted in the gas phase. Energies of optimized geometries are reported as free energies (G, kcal mol<sup>-1</sup>) with applied thermal and zero point corrections and are referenced relative to the  $\kappa^3$  intermediates that have the lowest barrier to formation (ring closure). No symmetry constraints were applied during optimization. Stationary points on the potential energy surface were identified as minima with no negative frequencies. Starting geometries for *N*-alkylated and -arylated five-coordinate structures were obtained by importing the Cartesian coordinates of crystallographically characterized products<sup>5</sup> into Gaussview and appending their ancillary groups as required. The *tert*-butyl groups on the ONO ligand backbone were simplified to hydrogens to reduce computational costs. Starting geometries for the octahedral intermediates were created by modifying crystal coordinates from homoleptic Si(ONO)<sub>2</sub>.<sup>5</sup> Transition state calculations for methyl and phenyl migration were performed initially with constrained Si–C and C–N distances, which were varied to locate the vicinity of the saddle points. A transition state search with relaxed constraints was subsequently performed to find the appropriate transition state. The transition states were confirmed to be saddle points in each case by the presence of a single imaginary frequency. Each transition state was verified to link the reactants and products by inspecting the trajectory of the normal mode corresponding to the imaginary frequency. Reported free energies use entropy corrections based on vibrational analyses carried out with the molecule embedded in the continuum solvent model. Plots of calculated Kohn–Sham orbitals were generated using Gaussview (v. 5.0.8) with an isovalue of 0.04.

For the Me(Ph)(Cl)Si(ONO) system, calculations were carried out with a larger basis set (6-311++G\*\*), using the M06 functional, and in the gas phase for comparison with the standard B3LYP/6-31G\*/PCM calculation. Calculations with additional polarization, diffuse functions, or using a different functional did not change the qualitative picture, and quantitative differences within the same reaction coordinate were almost always less than 2 kcal mol<sup>-1</sup>. (The sole exception is that treatment using the M06 functional resulted in a 5 kcal mol<sup>-1</sup> higher free energy for the  $\kappa^1$  reactant.) Continuum solvation results in stabilization of the  $\kappa^3$  isomers and the transition states forming them from the  $\kappa^1$  compound by 2–5 kcal mol<sup>-1</sup> relative to the other species and compared to gas-phase calculations, but the energy ordering of the transition states remains unchanged.

## ■ ASSOCIATED CONTENT

### ■ Supporting Information

Crystallographic information on Cl(Ph)Si(ON[Ph]O) in CIF format, summary of crystallographic details and selected metrical data, data on isomerization of five-coordinate silanes, and Cartesian coordinates of all calculated structures. This

material is available free of charge via the Internet at <http://pubs.acs.org>.

## ■ AUTHOR INFORMATION

### Corresponding Author

\*E-mail: Seth.N.Brown.114@nd.edu.

### Notes

The authors declare no competing financial interest.

## ■ ACKNOWLEDGMENTS

We thank Dr. Allen Oliver for his assistance with the X-ray crystallography. This work was supported by the National Science Foundation (CHE-1112356). Additional support from the Notre Dame Sustainable Energy Initiative is also gratefully acknowledged.

## ■ REFERENCES

- (1) Wuts, P. G. M.; Greene, T. W. *Greene's Protective Groups in Organic Synthesis*, 4th ed.; John Wiley & Sons: Hoboken, NJ, 2007.
- (2) (a) Corriu, R. *Pure Appl. Chem.* **1988**, *60*, 99–106. (b) Rendler, S.; Oestreich, M. *Synthesis* **2005**, 1727–1747.
- (3) (a) Hiyama, T. In *Metal Catalyzed Cross-Coupling Reactions*; Diederich, F., Stang, P. J., Eds.; Wiley-VCH: Weinheim, Germany, 1998; Chapter 10. (b) Denmark, S. E.; Sweis, R. F. *Acc. Chem. Res.* **2002**, *35*, 835–846.
- (4) (a) Jones, G. R.; Landais, Y. *Tetrahedron* **1996**, *52*, 7599–7662. (b) Mader, M. M.; Norrby, P.-O. *Chem.—Eur. J.* **2002**, *8*, 5043–5048.
- (5) Shekar, S.; Brown, S. N. *Organometallics* **2013**, *32*, 556–564.
- (6) (a) Camacho-Camacho, C.; Tlahuext, H.; Nöth, H.; Contreras, R. *Heteroat. Chem.* **1998**, *9*, 321–326. (b) Camacho-Camacho, C.; Mijangos, E.; Castillo-Ramos, M. E.; Esparza-Ruiz, A.; Vásquez-Badillo, A.; Nöth, H.; Flores-Parra, A.; Contreras, R. *J. Organomet. Chem.* **2010**, *695*, 833–840.
- (7) Walsh, R. *Acc. Chem. Res.* **1981**, *14*, 246–252.
- (8) Stegmann, H. B.; Scheffler, K.; Stöcker, F. *Angew. Chem., Int. Ed.* **1971**, *10*, 499–500.
- (9) (a) Stegmann, H. B.; Scheffler, K. *Chem. Ber.* **1970**, *103*, 1279–1285. (b) Uber, W.; Stegmann, H. B.; Scheffler, K.; Strähle, J. Z. *Naturforsch., B* **1977**, *32b*, 355–356.
- (10) Piskunov, A. V.; Sukhoshkina, O. Y.; Smolyanov, I. V. *Russ. J. Gen. Chem.* **2010**, *80*, 790–799.
- (11) Stegmann, H. B.; Scheffler, K.; Stöcker, F. *Angew. Chem., Int. Ed.* **1970**, *9*, 456.
- (12) Daikh, B. E.; Finke, R. G. *J. Am. Chem. Soc.* **1992**, *114*, 2938–2943.
- (13) Muetterties, E. L.; Mahler, W.; Schmutzler, R. *Inorg. Chem.* **1963**, *2*, 613–618.
- (14) Pastor, S. D.; Spivack, J. D.; Rodebaugh, R. K.; Bini, D. J. *Org. Chem.* **1984**, *49*, 1297–1300.
- (15) (a) Liepins, E.; Popelis, J.; Birgele, I.; Urtane, I.; Zelchan, G.; Lukevics, E. *J. Organomet. Chem.* **1980**, *201*, 113–121. (b) Kupče, E.; Liepiņš, E.; Lukevics, E. *J. Organomet. Chem.* **1983**, *248*, 131–147. (c) Pestunovich, V. A.; Lazareva, N. F.; Albanov, A. I.; Kozyreva, O. B.; Volkova, V. V.; Guseľ'nikov, L. E. *ARKIVOC* **2006**, 116–125.
- (16) Corriu, R. J. P.; Kpoton, A.; Poirier, M.; Royo, G.; Corey, J. Y. *J. Organomet. Chem.* **1984**, *277*, C25–C30.
- (17) Bento, A. P.; Solà, M.; Bickelhaupt, F. M. *J. Comput. Chem.* **2005**, *26*, 1497–1504.
- (18) Crouch, R. D. *Tetrahedron* **2004**, *60*, 5833–5871.
- (19) Ren, T. *Inorg. Chim. Acta* **1995**, *229*, 195–202.
- (20) (a) Ramsden, C. A. *Chem. Soc. Rev.* **1994**, *23*, 111–118. (b) Sidorkin, V. F.; Belogolova, E. F.; Pestunovich, V. A. *Russ. Chem. Bull.* **1998**, *47*, 225–230. (c) Couzijn, E. P. A.; Ehlers, A. W.; Schakel, M.; Lammertsma, K. *J. Am. Chem. Soc.* **2006**, *128*, 13634–13639. (d) Pierrefixe, S. C. A. H.; Bickelhaupt, F. M. *Struct. Chem.* **2007**, *18*, 813–819.



- (21) Harwood, L. M. *Polar Rearrangements*; Oxford University Press: New York, 1992.
- (22) Collins, C. J. *J. Am. Chem. Soc.* **1955**, *77*, 5517–5523.
- (23) (a) Ando, W.; Sekiguchi, A.; Migita, T. *Chem. Lett.* **1976**, 779–782. (b) Buynak, J. D.; Strickland, J. B.; Lamb, G. W.; Khasnis, D.; Modi, S.; Williams, D.; Zhang, H. *J. Org. Chem.* **1991**, *56*, 7076–7083. (c) Bakhtiar, R.; Holznagel, C. M.; Jacobson, D. B. *J. Am. Chem. Soc.* **1992**, *114*, 3227–3235. (d) Burger, P.; Bergman, R. G. *J. Am. Chem. Soc.* **1993**, *115*, 10462–10463. (e) Oku, A.; Miki, T.; Ose, Y. *J. Phys. Org. Chem.* **1996**, *9*, 619–622.
- (24) Protti, S.; Dondi, D.; Mella, M.; Fagnoni, M.; Albini, A. *Eur. J. Org. Chem.* **2011**, 3229–3237.
- (25) McGarvey, B. R.; Ozarowski, A.; Tian, Z.; Tuck, D. G. *Can. J. Chem.* **1995**, *73*, 1213–1222.
- (26) Sheldrick, G. M. *Acta Crystallogr.* **2008**, *A64*, 112–122.
- (27) *International Tables for Crystallography*; Kluwer Academic Publishers: Dordrecht, The Netherlands, 1992; C.
- (28) Frisch, M. J.; Trucks, G. W.; Schlegel, H. B.; Scuseria, G. E.; Robb, M. A.; Cheeseman, J. R.; Scalmani, G.; Barone, V.; Mennucci, B.; Petersson, G. A.; Nakatsuji, H.; Caricato, M.; Li, X.; Hratchian, H. P.; Izmaylov, A. F.; Bloino, J.; Zheng, G.; Sonnenberg, J. L.; Hada, M.; Ehara, M.; Toyota, K.; Fukuda, R.; Hasegawa, J.; Ishida, M.; Nakajima, T.; Honda, Y.; Kitao, O.; Nakai, H.; Vreven, T.; Montgomery, J. A., Jr.; Peralta, J. E.; Ogliaro, F.; Bearpark, M.; Heyd, J. J.; Brothers, E.; Kudin, K. N.; Staroverov, V. N.; Kobayashi, R.; Normand, J.; Raghavachari, K.; Rendell, A.; Burant, J. C.; Iyengar, S. S.; Tomasi, J.; Cossi, M.; Rega, N.; Millam, J. M.; Klene, M.; Knox, J. E.; Cross, J. B.; Bakken, V.; Adamo, C.; Jaramillo, J.; Gomperts, R.; Stratmann, R. E.; Yazyev, O.; Austin, A. J.; Cammi, R.; Pomelli, C.; Ochterski, J. W.; Martin, R. L.; Morokuma, K.; Zakrzewski, V. G.; Voth, G. A.; Salvador, P.; Dannenberg, J. J.; Dapprich, S.; Daniels, A. D.; Farkas, O.; Foresman, J. B.; Ortiz, J. V.; Cioslowski, J.; Fox, D. J. *Gaussian09*, revision A.02; Gaussian, Inc.: Wallingford, CT, 2009.